

## THE APPLICATION OF MICRO-RAMAN SPECTROSCOPY TO DISTINGUISH CARLOSTURANITE FROM SERPENTINE-GROUP MINERALS

ELENA BELLUSO<sup>§</sup>

*Dipartimento di Scienze Mineralogiche e Petrologiche e CNR, Istituto di Geoscienze e Georisorse, sez. di Torino, Via Valperga Caluso 35, I-10100 Torino, Italy*

ELISA FORNERO, SIMONA CAIRO, GIOVANNI ALBERTAZZI AND CATERINA RINAUDO

*Dipartimento di Scienze dell'Ambiente e della Vita, Via Bellini 25/g, I-15100 Alessandria, Italy*

### ABSTRACT

Carlosturanite, a mineral with a serpentine-like structure, grows mainly with a fibrous habit. We have analyzed samples with both pure carlosturanite and associations of carlosturanite and chrysotile using micro-Raman spectroscopy, a quick and non-destructive method of identifying different materials and mineral phases through direct analysis of bundles of fibers. Raman analysis was carried out on samples after first submitting them to chemical and mineralogical analysis using traditional techniques, *i.e.*, scanning electron microscopy (SEM) and transmission electron microscopy (TEM), with results evaluated in light of energy-dispersive spectrometry (EDS) and X-ray powder diffractometry (XRPD). This approach allowed us to determine the Raman spectrum associated with carlosturanite. Micro-Raman spectroscopy makes it possible to identify the different phases in these associations of minerals.

*Keywords:* carlosturanite, micro-Raman spectroscopy, transmission electron microscopy.

### SOMMAIRE

La carlosturanite, minéral ayant une structure semblable à celle d'une serpentine, croît surtout sous forme de fibres. Nous avons analysé des échantillons contenant la carlosturanite pure ou une association de carlosturanite et de chrysotile par spectroscopie micro-Raman, méthode rapide et non-destructive qui permet d'identifier des matériaux divers et des phases minérales par analyse directe de faisceaux de fibres. L'analyse Raman a porté sur des échantillons déjà analysés par méthodes traditionnelles, par exemple microscopie électronique à balayage, microscopie électronique par transmission, ces résultats étant évalués à la lumière de compositions obtenues par dispersion d'énergie et des spectres de diffraction obtenus sur poudre. Cette démarche nous a permis d'établir le spectre Raman de la carlosturanite. La spectroscopie micro-Raman permet l'identification de phases diverses dans ces associations de minéraux.

*Mots-clés:* carlosturanite, spectroscopie micro-Raman, microscopie électronique par transmission.

### INTRODUCTION

Carlosturanite is a rock-forming silicate found primarily in the Italian Western Alps (Belluso & Ferraris 1991, Compagnoni *et al.* 1985, Mellini *et al.* 1985); it has also been found in Taberg, Sweden (Mellini & Zussman 1986). It invariably appears in association with variable amounts of serpentine-group phases like chrysotile, fibrous antigorite and polygonal serpentine, protoserpentine (Baronnet & Belluso 2002) and other silicates growing with a fibrous habit, such as diopside,

forsterite, schorlomite (Alberico *et al.* 1993, Belluso & Ferraris 1991, Compagnoni *et al.* 1985). The chemical formula, determined by energy-dispersion analyses, shows that carlosturanite is poorer in Si and richer in H<sub>2</sub>O than the common serpentine-group phases (Compagnoni *et al.* 1985, Belluso & Ferraris 1991). On the basis of its chemical properties and results of a detailed investigation using high-resolution transmission electron microscopy (HRTEM), Mellini *et al.* (1985) proposed a structural model for carlosturanite based on the interruption of the phyllosilicate sheet of

<sup>§</sup> *E-mail address:* elena.belluso@unito.it

tetrahedra ( $T_2O_5$ ) and on the introduction of vacancies at tetrahedral sites along rows parallel to the direction of the  $TO_3$  chains. In this model, the sheet of octahedra of the serpentine structure is preserved, whereas one-seventh of the  $[Si_2O_7]^{6-}$  groups in the layer of tetrahedra is replaced by  $[(OH)_6H_2O]^{6-}$  groups substituting for oxygen atoms, bound to only one Si ion. The resulting layer of tetrahedra is thus formed of triple chains of tetrahedra bound to each other by means of  $H_2O$  molecules. As in the case of the serpentine-group phases, Mg, Fe, Mn, Ti and Cr ions may occur in the octahedral sites. Recent studies have shown that several serpentine-group phases and the mineral phases regulated as "asbestos" [anthophyllite, "amosite" (fibrous grunerite), actinolite, "crocidolite" (fibrous riebeckite) and tremolite, the quotation marks indicating non-approval by the IMA] can easily be distinguished on the basis of their Raman spectra (Rinaudo *et al.* 2003, 2004a), even where the minerals occur in association with other minerals (Rinaudo *et al.* 2005) or where they are analyzed in thin sections of rock (Groppo *et al.* 2006). In this work, micro-Raman spectroscopy is used on carlosturanite samples shown to be almost pure by scanning electron microscopy (SEM) and transmission electron microscopy (TEM), both equipped with energy-dispersive spectrometry (EDS), or in association with chrysotile. In this paper, we propose to establish the Raman spectrum of carlosturanite.

#### EXPERIMENTAL

All of the samples used in the study have an asbestiform habit and come from serpentinite outcrops in the Val Varaita region, in the Piedmont Region of northern Italy. Because of the usual intergrowth with other fibrous phases (Belluso & Ferraris 1991), the samples were first concentrated as much as possible by eliminating grains and fibers that did not appear golden brown by optical microscopy. Samples containing over 5% of mineral phases other than carlosturanite, as determined by X-ray powder diffraction (XRPD; Siemens D5000 diffractometer using  $CuK\alpha$  radiation), were excluded from the study. The morphological characteristics and elemental composition were determined using a SEM Cambridge Stereoscan 360 equipped with a Link Oxford Pentafet ATW2 analytical energy-dispersive microanalysis system (EDS).

The TEM characterization was performed either on crushed or on ion-thinned oriented specimens. We used a Philips CM12 instrument operated at 120 kV and equipped with an EDAX Si(Li) detector (located at the DSMP in Torino, Italy) and a JEOL 2000fx TEM operating at 200 kV and equipped with a Tracor TN 5502 EDX (located at CRMC-N in Luminy, Marseille, France). For the first type of analysis, samples were ground in an agate mortar with isopropyl alcohol, the suspension subjected to ultrasound treatment to minimize fiber aggregation, and several drops of the suspen-

sion were deposited onto a carbon film, supported on a Cu grid. For study with the JEOL, a 30  $\mu m$  section of the sample, cut normal to the elongation of the fiber bundle, was glued with Lakeside resin. A standard single-hole grid was glued onto a selected microdrilled area. The disk-grid assemblies were detached, washed and thinned with a Gatan 600 Duo Mill Ion operating with Ar at room temperature, 5 kV, 0.50 mA per gun,  $15^\circ$  and a finish angle of  $12^\circ$ .

Finally, two of the approximately thirty samples, hereafter referred to as samples 128 and 127, were selected for micro-Raman characterization; the first is almost pure carlosturanite, whereas the other contains other fibrous phases.

After being analyzed with SEM and TEM, the samples underwent micro-Raman characterization with a Jobin Yvon HR800 LabRam  $\mu$ -spectrometer equipped with an Olympus BX41 microscope, two interchangeable lasers, a standard laser (an HeNe 20 mW laser, 632.8 nm) and an external laser (a diode laser, 784.33 nm), and a CCD air-cooled detector. Calibration of the instrument was checked by noting the position of the Si band at  $\pm 520.6 \text{ cm}^{-1}$ . The spectra were acquired using a  $50\times$  lens, resulting in a laser beam-size on the sample of about 10  $\mu m$ , with a spectral resolution of  $1 \text{ cm}^{-1}$  and using 100 scans lasting 10 seconds each to optimize the signal-to-noise ratio. Only the spectral region from 1100 to  $300 \text{ cm}^{-1}$  was considered, because that is the area containing the lattice vibrational modes identified by Rinaudo *et al.* (2003) as characteristic for serpentine minerals and because a wide band due to fluorescence was observed at frequencies higher than  $1100 \text{ cm}^{-1}$ . The intense bands appearing to be asymmetrical were processed with the curve-fitting tool of the OPUS software program. Band fitting was carried out using a Gaussian function introducing the minimum number of component bands in the fitting process. Fitting was undertaken until reproducible results were obtained with the minimum residual error.

#### RESULTS AND DISCUSSION

In the SEM, all of the samples appear as bundles of single fibers strictly parallel to the fiber axis, *i.e.*, the [010] direction (Fig. 1). A TEM observation of sample 128 cut normal to the bundle axis showed grain sections appearing as polygons arranged in a mosaic texture, to form also triple junctions (Fig. 2). Our TEM-EDS analyses performed on the larger and best-developed crystals revealed a composition corresponding to carlosturanite (Table 1), with an empirical chemical formula (expressed as anhydrous compound):  $(Mg_{37.1}Ti_{2.0}Fe_{1.9}Mn_{0.5}Cr_{0.1})_{\Sigma 41.6}(Si_{22.4}Al_{1.0})_{\Sigma 23.4}O_{90}$ , which fits the expected ideal formula  $M_{42}T_{24}O_{56}(OH)_{68}(H_2O)_2$  proposed by Mellini *et al.* (1985).

In sample 127, the fibers appear larger and more irregular under the TEM, with a more irregular

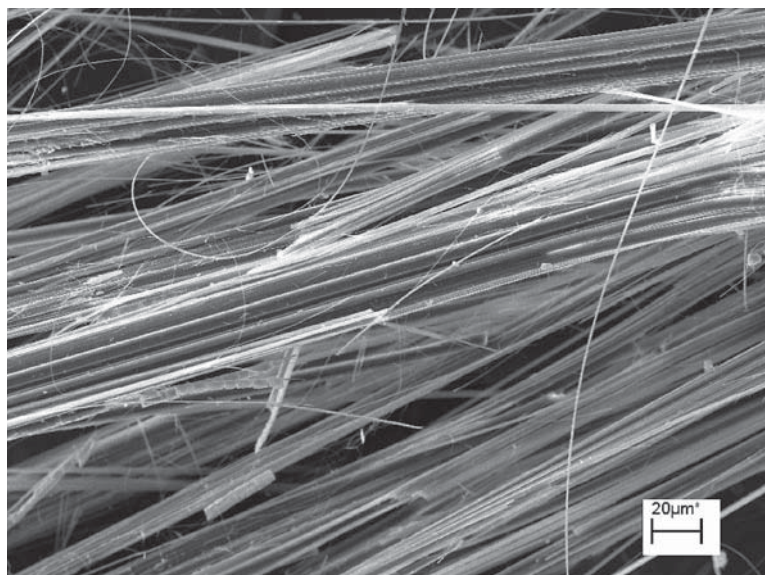


FIG. 1. Secondary electron image (SEM) of bundles of carlosturanite fibers showing the morphology of sample 128.

TABLE 1. TEM-EDS COMPOSITIONS CORRESPONDING TO CARLOSTURANITE IN SAMPLE 128

	1	2	3	4	5	6	7	8	9	10
Si <i>apfu</i>	22.3	22.4	22.1	23.1	21.8	21.8	22.3	21.8	22.4	22.7
Ti	1.9	2.4	2.0	2.0	2.1	1.8	2.0	2.3	2.1	2.0
Al	1.0	1.0	1.2	0.9	0.9	1.2	0.8	1.0	0.8	0.9
Fe <sup>2+</sup>	1.8	1.3	1.8	1.8	1.9	1.9	2.1	2.5	2.0	2.0
Mg	37.8	36.3	37.6	35.8	38.3	38.5	37.3	37.4	37.1	36.6
Mn	0.4	1.0	0.5	0.1	0.6	0.5	0.6	0.3	0.5	0.5
Cr	-	0.2	-	0.5	-	-	-	-	-	0.1

Cations normalization is based on 90 atoms of oxygen, considering carlosturanite as an anhydrous compound. Total iron is expressed as Fe<sup>2+</sup>.

cross-section of the single fibers as a result of a solid-state transformation of carlosturanite into chrysotile (Fig. 3).

A Raman analysis was first performed on the thicker and better-developed fibers of sample 128 (selected with the optical microscope attached to the spectrometer) to ensure that areas corresponding to carlosturanite were selected as the target of the micro-Raman beam. Numerous spectra were recorded. Figure 4 shows a typical Raman spectrum obtained on the type of fibers identified by SEM-EDS and TEM-EDS as carlosturanite in sample 128. On all the spectra recorded, fluorescence effects are observed in the portion of the spectrum corresponding to wavenumbers greater than 1100 cm<sup>-1</sup>; therefore, only the region of the spectrum ranging from 1100 and 300 cm<sup>-1</sup> has been taken into account. A characteristic broad band appears at 776 cm<sup>-1</sup> in the



FIG. 2. Medium-resolution TEM image of carlosturanite fibers in sample 128, as seen along the fiber axis, *i.e.*, the [010] direction.

Raman spectrum for carlosturanite; it is invariably the most intense band in the spectrum (Fig. 4). To rule out fluorescence effects as the cause of this band, spectra were recorded using 632.8 nm and 785.33 nm lasers as the excitation source. The wavelength and profile of the band were unaffected, indicating that the band is produced by vibrational modes. Recording spectra on a single fiber at different angles to the incident beam results in drastic changes in intensity; the band may therefore be assigned to symmetric modes. It lies at wavelengths greater than those detected as intense bands in the Raman spectra of the serpentine-group minerals studied, *e.g.*, chrysotile, antigorite and lizardite (Rinaudo *et al.* 2003). The deconvolution fitting program was applied to this part of the spectrum and, as expected, more than one band component can be identified. Figure 5 shows three separate bands at 788, 776 (the main band) and 765  $\text{cm}^{-1}$ . On all the spectra recorded, the form and wavelength of this band seem to define a fingerprint for carlosturanite. Analysis of other portions of the spectrum (Fig. 4) reveals three bands in the range from 720 to 600  $\text{cm}^{-1}$ , at 706, 692 and 671  $\text{cm}^{-1}$ . The frequencies of these bands are less characteristic. In fact, the symmetric stretching modes

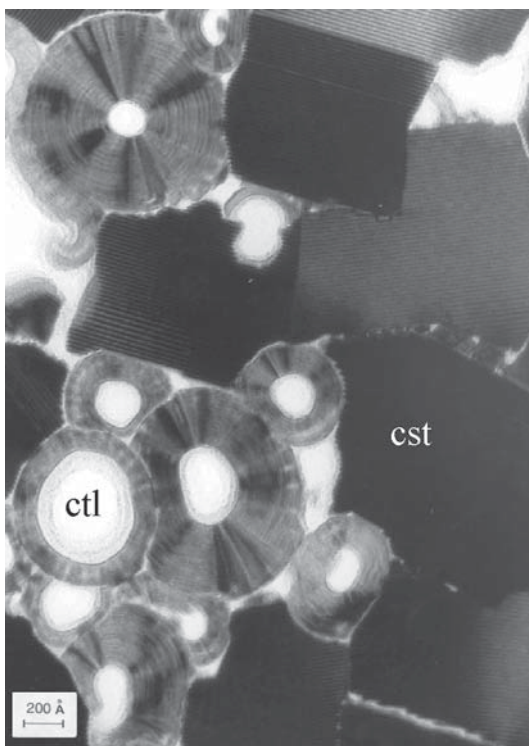


FIG. 3. Medium-resolution TEM image of sample 127, as seen normal to the fiber axis of the bundle and revealing carlosturanite (cst) with chrysotile (ctl).

( $\nu_s$ ) of the Si–O<sub>b</sub>–Si linkages are detected at 692  $\text{cm}^{-1}$  in chrysotile (Rinaudo *et al.* 2003), at  $675 \pm 1 \text{ cm}^{-1}$  in asbestiform tremolite and anthophyllite (Rinaudo *et al.* 2004a) and at  $704 \pm 3 \text{ cm}^{-1}$  in the dioctahedral phyllosilicates (Rinaudo *et al.* 2004b). The same assignment,  $\nu_s$  modes of the Si–O<sub>b</sub>–Si linkages, may be proposed for the three bands at 671, 692 and 706  $\text{cm}^{-1}$  in carlosturanite. On the other hand, in the crystalline structure of carlosturanite, as described by Mellini *et al.* (1985), two structural components can be identified, one attributed to a phyllosilicate module, where the different TO<sub>4</sub> share three corners with other tetrahedra,

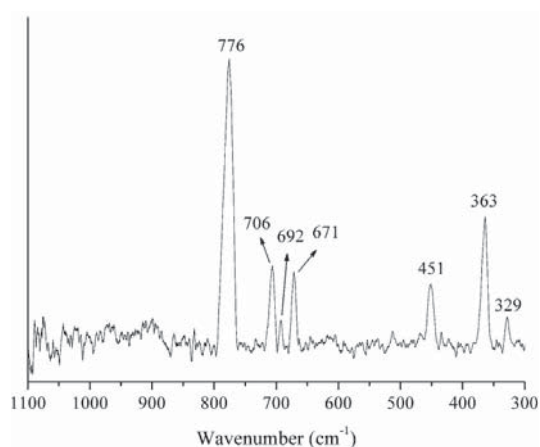


FIG. 4. Typical micro-Raman spectrum of sample 128 registered on the bundles of fibers, identified by TEM-EDS as carlosturanite.

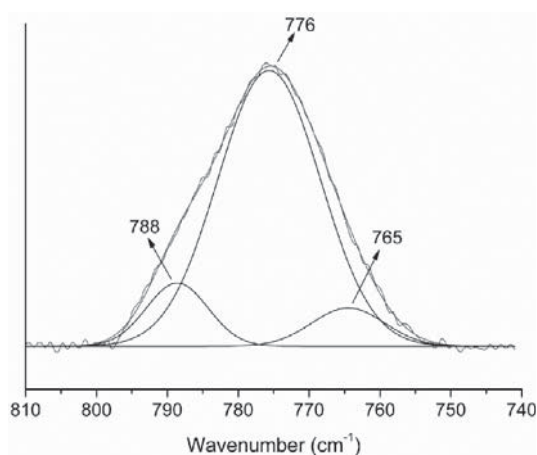


FIG. 5. Deconvolution of the band at 776  $\text{cm}^{-1}$  in Figure 4; three component bands are identified, at 788, 776 and 765  $\text{cm}^{-1}$ .



and another one attributable to an amphibole module, where the  $TO_4$  groups share only two corners with contiguous tetrahedra. Furthermore, the presence of Fe [which in carlosturanite is, according to Deriu *et al.* (1994), 38%  $Fe^{3+}$  of the total Fe], Ti, and Cr replacing Mg in the octahedral sites makes some parts of the carlosturanite structure dioctahedral. It is therefore not surprising that the  $\nu_s$  modes of the tetrahedra, differing from the structural point of view, vibrate at the wavelengths typical for the phyllosilicate and amphibole structural components. It is more difficult to attribute the intense band at  $776\text{ cm}^{-1}$ ; normally, the vibrations of the octahedrally coordinated Mg or Al ions, linked to  $OH^-$  groups, are found at these wavelengths in the serpentine phases, but there they appear as very broad and weak bands (Farmer 1974, Rinaudo *et al.* 2004b). In the carlosturanite spectrum, in contrast, this band is the most intense and is therefore probably related to vibrations of the groups lying near the interrupted silicate layers, where the  $[(OH)_6H_2O]^{6-}$  groups form the peculiarity of the mineral's structure. Final assignment of this band will be possible only once the vibrational spectrum has been calculated on the basis of more conclusive structural data.

As for the lower part of the spectrum, three bands are detected in the  $500\text{--}300\text{ cm}^{-1}$  frequency range (Fig. 4). Among these, the band at  $363\text{ cm}^{-1}$  is very intense in all the spectra recorded, and may correspond to  $\nu_5(e)$  vibrational modes of the  $TO_4$  tetrahedra. In the Raman spectra of the serpentine-group minerals, these modes generate an intense band at a slightly higher wavelength, *i.e.*,  $375\text{--}380\text{ cm}^{-1}$  (Rinaudo *et al.* 2003, Kloprogge *et al.* 1999). By analogy, the band at  $451\text{ cm}^{-1}$  may be

produced by the  $\nu_3(a_1)$  vibrational modes of the  $TO_4$  tetrahedra, which vibrate in the chrysotile structure at  $458\text{ cm}^{-1}$  (Kloprogge *et al.* 1999).

Turning to sample 127, Figure 6 shows a typical Raman spectrum recorded on a sample on which SEM-EDS analyses and TEM observations revealed both carlosturanite and chrysotile (Fig. 3). The Raman spectrum of Figure 6 indicates that in these samples also, the most intense band lies at  $774\text{ cm}^{-1}$  and is broad. The component bands lie at  $786$ ,  $773$  (the main) and  $762\text{ cm}^{-1}$  (Fig. 7) or, in other words,  $3\text{ cm}^{-1}$  lower than those detected in sample 128 (Fig. 5). The band at  $694\text{ cm}^{-1}$  is also invariably broader, and thus formed by at least two components, identified with the fitting program at  $694$  and  $704\text{ cm}^{-1}$  (Fig. 8), corresponding to wavelengths at which distinct bands are observed on the Raman spectrum from pure carlosturanite (Fig. 4). The intensity of the band at  $692 \pm 2\text{ cm}^{-1}$  in the Raman spectra of samples 127 and 128 is different. With pure carlosturanite (Fig. 4), the band is invariably weak in intensity, whereas in the spectra from sample 127, it is invariably strong (Figs. 6, 8). The other Raman bands in sample 127 (Fig. 6) are a good match for those observed in carlosturanite (Fig. 4), with the exception of a band at  $391\text{ cm}^{-1}$ , which does not appear in the spectrum of this mineral.

The strong intensity of the band at  $694\text{ cm}^{-1}$  and the presence of the band at  $391\text{ cm}^{-1}$  in sample 127 may be related to the presence of chrysotile, in which the  $\nu_s$  modes of the Si-O<sub>b</sub>-Si linkages lie at  $692\text{ cm}^{-1}$  and the  $\nu_5(e)$  vibrational modes of the  $TO_4$  tetrahedra are found at  $389\text{ cm}^{-1}$  (Rinaudo *et al.* 2003). The consequence of the high intensity of the band at  $694\text{ cm}^{-1}$ , produced by both chrysotile and carlosturanite, makes this part of the spectrum convoluted. The band at  $704\text{ cm}^{-1}$  produced

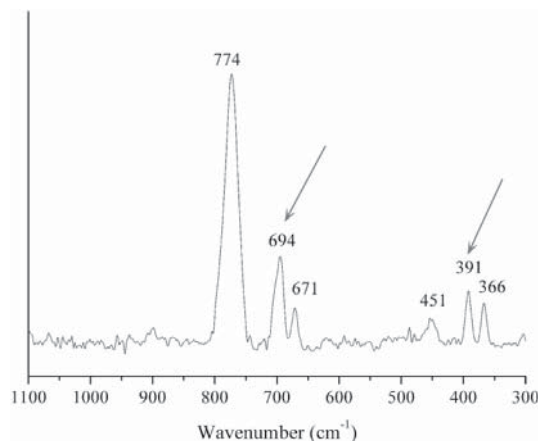


FIG. 6. Typical Raman spectrum of sample 127. The presence of chrysotile in the sample is confirmed by the band at  $391\text{ cm}^{-1}$  and the higher intensity of the band at  $694\text{ cm}^{-1}$ , characteristics of this mineral. In sample 128, the first band is not observed, and the second one shows a weak intensity.

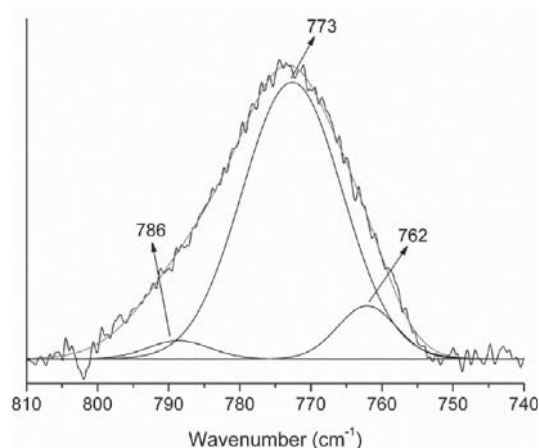


FIG. 7. Deconvolution of the band at  $774\text{ cm}^{-1}$  for sample 127, registered in Figure 6. Three component bands are identified, at  $786$ ,  $773$  and  $762\text{ cm}^{-1}$ .

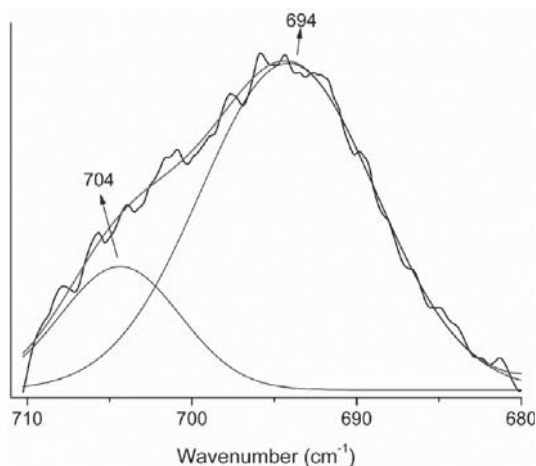


FIG. 8. Deconvolution of the band at  $694\text{ cm}^{-1}$  detected in the spectra obtained from sample 127. Two component bands are detected, at  $694$  and  $704\text{ cm}^{-1}$ .

by carlosturanite may be placed in evidence only when fitting of the band is performed. Several Raman spectra of sample 127 have been recorded, and the result invariably indicates the presence of two phases: carlosturanite and chrysotile.

#### CONCLUSIONS

On the basis of this study, we conclude that the Raman spectrum of the phase carlosturanite is characterized by a main band at  $775 \pm 1\text{ cm}^{-1}$ , which can be considered as a fingerprint for carlosturanite, allowing it to be identified in natural associations. Moreover, our results confirm the earlier findings of our group (Rinaudo *et al.* 2003, 2004a, 2005, Groppo *et al.* 2006): Raman spectroscopy is a powerful tool for the identification of mineral phases once the Raman spectrum of the pure phase has been determined.

#### ACKNOWLEDGEMENTS

The authors thank Alain Baronnet, S. Nitsche and F. Quintric of C.R.M.C.N. in Luminy, Marseille, France, for allowing use of their laboratory's TEM-EDS equipment and photographic facilities, Prof. Marcello Mellini, an anonymous referee and Associate Editor Roberta Flemming for their helpful suggestions. The financial support of the Ministero dell'Università e della Ricerca is gratefully acknowledged (PRIN 2004 project: "Spectroscopic and computational characterization of fibrous minerals not classified as asbestos").

#### REFERENCES

- ALBERICO, A., BELLUSO, E., COMPAGNONI, R. & FERRARIS, G. (1993): Schorlomite fibrosa in vene a carlosturanite entro le serpentiniti ofiolitiche della Val Varaita (Alpi Occidentali). *Plinius* **14**, 28-29.
- BARONNET, A. & BELLUSO, E. (2002): Microstructures of the silicates: key information about mineral reactions and a link with the Earth and materials sciences. *Mineral. Mag.* **66**, 709-732.
- BELLUSO, E. & FERRARIS, G. (1991): New data on balangeroite and carlosturanite from Alpine serpentinites. *Eur. J. Mineral.* **3**, 559-566.
- COMPAGNONI, R., FERRARIS, G. & MELLINI, M. (1985): Carlosturanite, a new asbestiform rock-forming silicate from Val Varaita, Italy. *Am. Mineral.* **70**, 767-772.
- DERIU, A., FERRARIS, G. & BELLUSO, E. (1994):  $^{57}\text{Fe}$  Mössbauer study of the asbestiform silicates balangeroite and carlosturanite. *Phys. Chem. Minerals* **21**, 222-227.
- FARMER, V.C. (1974): *The Infrared Spectra of Minerals*. Mineralogical Society, London, U.K.
- GROPPA, C., RINAUDO, C., CAIRO, S., GASTALDI, D. & COMPAGNONI, R. (2006): Micro-Raman spectroscopy for a quick and reliable identification of serpentine minerals from ultramafics. *Eur. J. Mineral.* **18**, 319-329.
- KLOPPROGGE, J.T., FROST, R.L. & RINTOUL, L. (1999): Single crystal Raman microscopic study of the asbestos mineral chrysotile. *Phys. Chem., Chem. Phys.* **1**, 2559-2564.
- MELLINI, M., FERRARIS, G. & COMPAGNONI, R. (1985): Carlosturanite: HRTEM evidence of a polysomatic series including serpentine. *Am. Mineral.* **70**, 773-781.
- MELLINI, M. & ZUSSMAN, J. (1986): Carlosturanite (not "picrolite") from Taberg, Sweden. *Mineral. Mag.* **50**, 675-679.
- RINAUDO, C., BELLUSO, E. & GASTALDI, D. (2004a): Assessment of the use of Raman spectroscopy for the determination of amphibole asbestos. *Mineral. Mag.* **68**, 455-465.
- RINAUDO, C., GASTALDI, D. & BELLUSO, E. (2003): Characterization of chrysotile, antigorite and lizardite by FT-Raman spectroscopy. *Can. Mineral.* **41**, 883-890.
- RINAUDO, C., GASTALDI, D., BELLUSO, E. & CAPELLA, S. (2005): Application of Raman spectroscopy on asbestos fibre identification. *Neues Jahrb. Mineral., Abh.* **182**, 31-36.
- RINAUDO, C., ROZ, M., BOERO, V. & FRANCHINI-ANGELA, M. (2004b): FT-Raman spectroscopy on several di- and tri-octahedral T-O-T phyllosilicates. *Neues Jahrb. Mineral., Monatsh.*, 537-554.

Received January 11, 2007, revised manuscript accepted March 31, 2007.